

RESEARCH ARTICLE

Revealing the high variability on nonconserved core and mobile elements of *Austropuccinia psidii* and other rust mitochondrial genomes

Jaqueline Raquel de Almeida¹, Diego Mauricio Riaño Pachón², Livia Maria Franceschini¹, Isanelli Batista dos Santos¹, Jessica Aparecida Ferrarezi¹, Pedro Avelino Maia de Andrade¹, Claudia Barros Monteiro-Vitorello¹, Carlos Alberto Labate¹, Maria Carolina Quecine^{1*}

1 Department of Genetics, “Luiz de Queiroz” College of Agriculture (ESALQ), University of São Paulo, Piracicaba, São Paulo, Brazil, **2** Center for Nuclear Energy in Agriculture (CENA), University of São Paulo, Piracicaba, São Paulo, Brazil

* mquecine@usp.br



OPEN ACCESS

Citation: de Almeida JR, Riaño Pachón DM, Franceschini LM, dos Santos IB, Ferrarezi JA, de Andrade PAM, et al. (2021) Revealing the high variability on nonconserved core and mobile elements of *Austropuccinia psidii* and other rust mitochondrial genomes. PLoS ONE 16(3): e0248054. <https://doi.org/10.1371/journal.pone.0248054>

Editor: Minou Nowroussian, Ruhr-Universität Bochum, GERMANY

Received: August 24, 2020

Accepted: February 18, 2021

Published: March 11, 2021

Peer Review History: PLOS recognizes the benefits of transparency in the peer review process; therefore, we enable the publication of all of the content of peer review and author responses alongside final, published articles. The editorial history of this article is available here: <https://doi.org/10.1371/journal.pone.0248054>

Copyright: © 2021 de Almeida et al. This is an open access article distributed under the terms of the [Creative Commons Attribution License](https://creativecommons.org/licenses/by/4.0/), which permits unrestricted use, distribution, and reproduction in any medium, provided the original author and source are credited.

Data Availability Statement: The complete sequence of the mitochondrial genome of *A. psidii*

Abstract

Mitochondrial genomes are highly conserved in many fungal groups, and they can help characterize the phylogenetic relationships and evolutionary biology of plant pathogenic fungi. Rust fungi are among the most devastating diseases for economically important crops around the world. Here, we report the complete sequence and annotation of the mitochondrial genome of *Austropuccinia psidii* (syn. *Puccinia psidii*), the causal agent of myrtle rust. We performed a phylogenomic analysis including the complete mitochondrial sequences from other rust fungi. The genome composed of 93,299 bp has 73 predicted genes, 33 of which encoded nonconserved proteins (ncORFs), representing almost 45% of all predicted genes. *A. psidii* mtDNA is one of the largest rust mtDNA sequenced to date, most likely due to the abundance of ncORFs. Among them, 33% were within intronic regions of diverse intron groups. Mobile genetic elements invading intron sequences may have played significant roles in size but not shaping of the rust mitochondrial genome structure. The mtDNAs from rust fungi are highly syntenic. Phylogenetic inferences with 14 concatenated mitochondrial proteins encoded by the core genes placed *A. psidii* according to phylogenetic analysis based on 18S rDNA. Interestingly, *cox1*, the gene with the greatest number of introns, provided phylogenies not congruent with the core set. For the first time, we identified the proteins encoded by three *A. psidii* ncORFs using proteomics analyses. Also, the *orf208* encoded a transmembrane protein repressed during *in vitro* morphogenesis. To the best of our knowledge, we presented the first report of a complete mtDNA sequence of a member of the family Sphaerophragmiacea.

has been deposited in GenBank (accession number MN018834).

Funding: This study was supported by Fundação de Amparo à Pesquisa do Estado de São Paulo FAPESP (Grant 2014/16804-4). We thank FAPESP for the fellowship award to JRA (2016/16868-8) and LMF (2015/14344-9). We also thank Coordenação de Aperfeiçoamento de Pessoal de Nível Superior (CAPES) for the fellowship award to IBS and Conselho Nacional de Desenvolvimento Científico e Tecnológico (CNPq) to JAF and PAMA.

Competing interests: The authors have declared that no competing interests exist.

Introduction

Rust fungi, classified as the most devastating diseases worldwide, are widely distributed in nature [1]. *Austropuccinia psidii* [2,3] is an obligate biotrophic plant pathogen that is the causal agent of myrtle rust. This pathogen has evolved specialized structures, such as haustoria, formed within the host tissue to efficiently acquire nutrients and suppress host defenses [4,5].

Myrtle rust, first described as occurring on leaves of *Psidium guajava* L. (*Psidium pomiferum* L.) (Myrtaceae) in Brazil [2], can now infect various species within the genus *Eucalyptus* [6,7]. Quecine *et al.* [8] suggested that it is most likely due to its high genetic variability within populations [8]. In South America, rust is a significant threat to *Eucalyptus grandis*, one of the most cultivated species. Moreover, it is becoming significant to Myrtle species in its origin center Australia. To date, 358 native species from 49 genera identified in Australia were susceptible to rust [9]. There are several efforts to improve knowledge about the biology of *A. psidii*, such as the sequencing of its nuclear genome [10–13]; proteomic of urediniospores [14]; effects of cuticular waxes on fungal germination [15]; confirmation of its sexual life cycle [12,16]; among others. Recently, taxonomic studies have led to the reclassification of *A. psidii*. A maximum-likelihood phylogenetic analysis using the sequences of the nuclear ribosomal RNA genes suggested that *A. psidii* does not belong to *Puccinia* but should be within the new genus *Austropuccinia* of Pucciniales in the redefined family Sphaerophragmiaceae [3].

Fungal mitochondrial genomes are typically small, circular, and double-stranded DNA molecules. These genomes usually harbor at least 14 protein-coding conserved genes, namely, apocytocrome b (*cob*); three subunits of the cytochrome c oxidase (*cox1*, *cox2*, *cox3*); seven subunits of the NADH subunits (*nad1*, *nad2*, *nad3*, *nad4*, *nad4L*, *nad5*, and *nad6*); three subunits of the ATP synthase (*atp6*, *atp8*, *atp9*); as well as the large and small ribosomal RNA (rRNA) subunits (*rnl* and *rns*); a set of tRNAs genes; and the RNA subunit of the mitochondrial RNase P (*rnpB*). The genomes also present a variable number of groups-I and -II introns that may bear homing endonuclease genes (HEGs) with LAGLIDADG or GIY-YIG motifs [17–19]. HEGs are selfish genetic mobile elements that encode site-specific-sequence-tolerant DNA endonucleases. The catalytic activity of HEGs promotes their propagation by introducing DNA double-strand breaks (DSBs) into alleles lacking the endonuclease-coding sequence and by the subsequent repair of these DSBs via homologous recombination using the endonuclease-containing allele as a template [20]. mtDNA also harbors numerous repetitive sequences, besides introns and plasmids, known as mtDNA instability agents, generating variability within fungal mitochondrial genomes [21,22]. According to Kolesnikova *et al.* [23], the variation in mtDNA size in four different *Armillaria* species is due to variable numbers of mobile genetic elements, introns, and plasmid-related sequences. Most *Armillaria* introns contained open reading frames (ORFs) related to homing endonucleases of the LAGLIDADG and GIY-YIG families.

Mitochondrial genomes evolve independently of and faster than the nuclear genome [24]. It is often useful as a valuable source of information to study systematics and evolutionary biology in eukaryotes where insufficient phylogenetic signals have accumulated in nuclear genes [17,25]. For instance, Song *et al.* [26] resolved some incongruences of Dothideomycetes phylogeny using the mitochondrial genome of many phytopathogens belonging to this Class [26]. The availability of mitochondrial genome sequences provides valuable information about genome organization and enables evaluating structural rearrangements using comparative studies [27]. The high rate of polymorphism frequently found within introns or intergenic regions of well-conserved mitochondrial genes makes these sequences useful for genetic diversity studies, both among and within populations [28–31].

In addition to its role in energy production and other essential cellular processes, mitochondria may also participate in fungal pathogenesis [25]. For instance, mitochondrial β -

oxidation plays an essential role in vegetative growth, conidiation, appressorial morphogenesis, and pathogenesis progression in *M. oryzae* [31]. The methylation of the mitochondrial genome is an epigenetic mechanism affecting the adaptation and pathogenicity of *Candida albicans* [32]. Furthermore, mitochondrial metabolic functions are targets for pathogen control [33,34].

Based on the critical role of mitochondria to phytopathogenic fungi and the need to better understand the myrtle rust causal agent, we sequenced, assembled, and annotated the *A. psidii* mitochondrial genome. We thoroughly characterized the genome's gene content and organization, codon usage, and repetitive elements. We also explored the evolutionary dynamics of the mitochondrial genomes of rust fungi by a comparative mtDNA focused on mobile element analysis. Finally, through proteomic approaches, we identified three previously hypothetical mitochondrial proteins unique to *A. psidii*.

Materials and methods

DNA sequencing and mitochondrial genome assembly

A. psidii monopustular isolate MF-1 was previously obtained from *E. grandis* [35]. The high-molecular-weight DNA of MF-1 was obtained from urediniospores using the DNeasy Plant mini kit (Qiagen). A NanoVue spectrophotometer quantified the extracted DNA, and the quality was checked by agarose gel electrophoresis. Total DNA was used to generate libraries for 454 pyrosequencing (Roche), PacBio SMRT sequencing on an RSII instrument (Pacific Biosciences), and sequencing by synthesis on a MiSeq Instrument (Illumina).

We obtained *A. psidii* mtDNA sequences by mining reads from 454 and MiSeq platforms using mitochondrial reference genomes.

Complete mitochondrial genome sequences from all available species of representative rust fungi (Pucciniales) were obtained from the NCBI database and Puccinia's comparative genomics projects of the Broad Institute (Table 1).

Mining was performed using the Mirabait program in the MIRA package using the MITO-bim approach. All steps were performed using modules of the MIRA sequence assembler software in "mapping mode" to map reads to a reference and create new reference sequences; and an in silico-baiting module, which is used to extract reads that precisely match a given reference across a number of n k -mers of length k (defaults $n = 1$ and $k = 31$) from the entire set of reads [36]. Finally, mitochondrial reference genomes were used to mapping single molecule

Table 1. Complete mitochondrial genome of rust pathogens used in present work.

Reference organisms	Data source *	Pathogen's characteristics
<i>Phakopsora meibomia</i> Puerto_Rico	NCBI (NC_014352.1)	Causal agent of American rust. It occurs mainly in soybean crops.
<i>Phakopsora pachyrhizi</i> Taiwan_72-1	NCBI (NC_014344.1)	Causal agent of Asian soybean rust. It occurs mainly in soybean crops.
<i>Puccinia graminis</i> f. sp. <i>tritici</i>	<i>Puccinia</i> —Group Database Broad Institute	Causal agent of stem rust. It occurs in wheat, barley, rye, triticale and some other species of Poaceae (Gramineae).
<i>Puccinia striiformis</i> PST-78	<i>Puccinia</i> —Group Database Broad Institute	Causal agent of wheat yellow rust, which occurs in crops of wheat and barley.
<i>Puccinia triticina</i> 1-1BBBD-race-1	<i>Puccinia</i> —Group Database Broad Institute	Causal agent of wheat leaf rust.
<i>Moniliophthora perniciosa</i>	NCBI (NC_005927.1)	Causal agent of "witches' broom disease" of the cocoa tree.

**Puccinia*—Group Database Broad Institute http://www.broadinstitute.org/annotation/genome/puccinia_group/MultiHome.html.

NCBI - <http://www.ncbi.nlm.nih.gov/>.

<https://doi.org/10.1371/journal.pone.0248054.t001>

sequencing reads from SMRT platform using basic local alignment using BlasR package (<https://github.com/PacificBiosciences/blasr>) developed by PacificBioscience [37].

The assembly of the *A. psidii* mitochondrial genome from reads and subreads of MiSeq, 454, and SMRT platforms were performed using SPAdes v. 3.7 (<http://cab.spbu.ru/files/release3.7.0/manual.html>) with automatic coverage cutoff [38]. QUAST v. 4.0 (<http://bioinf.spbau.ru/quast>) was used to compute assembly metrics and validate assembly quality [39,40]. All computational analyses were performed according to software tutorials.

Annotation of the mitochondrial genome

A. psidii mitochondrial genome was annotated using the default parameters of MFannot (<https://github.com/BFL-lab/Mfannot>) [41] and GeSeq (<https://chlorobox.mpimp-golm.mpg.de/geseq.html>) [42]. The annotation was adjusted manually using the BLASTx tool available in the NCBI, restricting the similarity search to the "Pucciniales" order (taxid:5258). The Genome Vx tool (<http://wolfe.ucd.ie/GenomeVx/>) was used to plot each gene's position and orientation from the mitochondrial genome of *A. psidii*.

For the identification of the transfer RNAs (tRNAs), the tRNAscan-SE software (<http://lowelab.ucsc.edu/tRNAscan-SE/>) was used with default parameters [43]. The GC content analysis of the mitochondrial genome was performed with program Genomics % GC Content Calculator (http://www.sciencebuddies.org/science-fair-projects/project_ideas/Genom_GC_Calculator.shtml).

The complete sequence of the mitochondrial genome of *A. psidii* was deposited in GenBank (accession number MN018834).

Comparative and phylogenetic analysis of rust mtDNAs

Comparative and phylogenetic analyses were performed among the rust mtDNA from *A. psidii*, *P. graminis f. sp. tritici*, *P. triticina*, *P. striiformis*, *P. meibomiaae*, and *P. pachyrhizi* (Table 1). The mitochondrial genome sequence of *Moniliophthora perniciosa* (NC_005927.1) was used as an outgroup [44]. The mitochondrial genomes of *P. graminis f. sp. tritici*, *P. triticina*, and *P. striiformis*, *P. meibomiaae*, *P. pachyrhizi*, *M. perniciosa* were reannotated using MFannot and GeSeq and manually verified to avoid errors in comparative and phylogenetic analyses. The nonconserved ORF (ncORFs) from all mtDNA rust fungi were annotated by BLAST analysis. We defined as ncORFs all predicted ORFs that did not belong to the mitochondrial core protein-encoding genes. We also used the tRNAscan-SE software and Genomics % GC Content Calculator to identify tRNAs and GC% content in the rust mtDNAs.

The fourteen conserved mitochondrial protein sequences were used for phylogenetic analyses: cytochrome c oxidase (*cob*, *cox1*, *cox2*, *cox3*), ATP synthase subunits (*atp6*, *atp8*, *atp9*), and NADH dehydrogenase subunits (*nad1*, *nad2*, *nad3*, *nad4*, *nad4L*, *nad5*, and *nad6*). Protein sequences were aligned with MUSCLE implemented in MEGA X [45]. Poorly aligned amino acid regions were removed using TrimAl (<http://trimal.cgenomics.org/>) [46]. Proper evolutionary models for phylogenetic inference were computed with MrModeltest v. 2.3 (<https://github.com/nylander/MrModeltest2>) [47] using the Bayesian Information Criterion (BIC). Specifically, mtREV24 was determined as the best model for *cob*, LG+I+F for *cox1*, cpREV for *cox2*; WAG+I+F for *cox3*; mtREV24+G for *atp6*; mtREV24 for *atp8*; mtREV24+I for *atp9*; mtREV24 for *nad1*; WAG+I+F for *nad2*; mtREV24+G for *nad3*; JTT+I+F for *nad4*, cpREV for *nad4L*; WAG+G+I+F for *nad5*; JTT+G+F for *nad6*. The 14 protein sequences of each pathogen were concatenated using Mesquite software v. 3.2 (<https://www.mesquiteproject.org/>) [48], and Bayesian phylogenetic inference was carried out with MrBayes v. 3.2.7 (<https://nbisweden.github.io/MrBayes/download.html>). The Bayesian analysis included two separate

runs of 1×10^7 generations, sampled every 1000 generations, and 25% of the initial generations.

In addition, the phylogenetic relationship of *A. psidii* within rust fungi was evaluated using the 18S rDNA and *cox1* genes. Multiple sequence alignments were generated with MUSCLE [49], trimmed with TrimAl, and selected the best evolutionary model described above (LG+I+F for *cox1*, T92+G+I for 18S rDNA). The phylogenetic tree was inferred as previously mentioned using MrBayes.

Proteomics analysis

Data processing, protein identification, and relative quantitative analyses of proteomics data were performed using the raw data previously obtained by Quecine *et al.* [14] using the ProteinLynx Global Server (PLGS- v 2.5.1). The reanalysis of the *A. psidii* proteome was performed to validate the presence of hypothetical proteins in the *A. psidii* mitochondrial genome. The processing parameters were set, according to Quecine *et al.* [14]. Briefly, to identify the proteins, the intensities of the spectra were calculated by the stoichiometric method, according to the internal standard, the sequence of rabbit phosphorylase (Uniprot entry: P00489), by MSE analysis [50] and normalized using the PLGS auto normalization function. Protein identifications were obtained with the embedded ion accounting algorithm of PLGS software searching into the *A. psidii* mitochondrial proteins appended in the internal standard. All protein hits were identified with confidence of >95%.

A database was created based on the predicted proteins obtained from the manual annotation of the mitochondrial genome of *A. psidii*, as well as on mitochondrial protein sequences of *P. graminis* f. sp. *tritici*, *P. triticina*, *P. striiformis* (Broad Institute's Puccinia—Group Database). Protein identification was obtained with the embedded ion accounting algorithm of PLGS software. After PLGS 2.5.1 analysis, the data were manually inspected, and the parameters obtained using MassPivot v. 101 were included: (i) the average amount (fmol) of protein, (ii) the average score of proteins, and (iii) the average amount of matched peptides to each protein.

For the hypothetical proteins found on the proteomics data, we performed additional in silico analyses. The peptide sequences were obtained by EMBOSS Transeq (https://www.ebi.ac.uk/Tools/st/emboss_transeq/) and then the conserved motifs evaluated by MOTIF, Genome-Net of the Kyoto University Bioinformatics Center (<http://www.genome.jp/tools/motif/>).

RT-qPCR analysis

To validate the proteomic analysis, gene expression of the three ncORFs, *orf174*, *orf205*, *orf208*, identified by mass spectrometry, was evaluated by RT-qPCR during the fungal in vitro morphogenesis as described below. The set of primers for ncORFs was generated using Oligo-Perfect™ Designer software (<http://tools.lifetechnologies.com/content>). The presence of dimers and hairpins was verified using Oligo Analysis Tool software (<http://www.operon.com/tools/oligo-analysisistool.aspx>). The genes of beta-tubulin and elongation factor were used as references [51] (Table 2).

In vitro morphogenesis experiment: *A. psidii* urediniospores from the monopustular isolate MF-1 were inoculated on dialysis membranes on agar-water medium (8 g L^{-1}) amended with 0.5% of olive oil [52,53]. Dialysis membranes were sampled at each interval: zero hours after inoculation (h.a.i.), 6 h.a.i. (absence of germination), 12 h.a.i. (germination tubes formation), and 24 h.a.i. (appressoria formation) [35]. Total RNA of four biological replicates for each time was isolated using a spin column procedure employing a Spectrum Plant Total RNA Extraction Kit (Sigma-Aldrich). RNA isolation procedure followed the manufacturer's

Table 2. Primers used in this study.

Target gene	Primer	Sequence 5'- 3'	Reference
<i>beta-tubulin</i>	BTub1	GGACTCTGTTTTAGATGTCGTC	Bini <i>et al.</i> 2017
	BTub3	TTGATGGACTGATAGGGTAGCG	Bini <i>et al.</i> 2017
<i>elongation factor</i>	EF5	CAGTTATGGAAGTTTGAAACTCC	Bini <i>et al.</i> 2017
	EF2	GACAATAAGCTGTGCAACACCAAGG	Bini <i>et al.</i> 2017
<i>orf174</i>	Po174F	GGCACACGACCTCTGTACCT	This study
	Po174R	TTCACAAGATGCAGGCTCAC	This study
<i>orf205</i>	Po205F	TGCAGAGAAGGATGCACAAC	This study
	Po205R	TCAAAAGCATGAACCATTCG	This study
<i>orf208</i>	Po208F	GAAGGTAAGCGGGAGGGTA	This study
	Po208R	TTCTACCCCGTTCTATTCTATCC	This study

<https://doi.org/10.1371/journal.pone.0248054.t002>

protocol, including on-column DNase digestion (Sigma-Aldrich). RNA concentration and A260/A280 ratios were measured for each sample by a NanoVue Spectrophotometer (GE Healthcare). Quantified RNA samples were stored at -80°C. One µg of each RNA sample was reverse-transcribed to cDNA using a High Capacity cDNA Reverse Transcription Kit (Applied Biosystems, Foster City, USA), employing random hexamer primers. Reverse-transcribed samples were stored at -20°C. The RT-qPCR reactions were prepared in a final volume of 12.5 µl containing 6.25 µl of Platinum® SYBR® Green qPCR SuperMix-UDG, 10 pmol of each primer set, 2.5 µl cDNA (1:20) and 1.75 µl ultrapure water. The samples were amplified in an iCycler IQ® Real-Time PCR Detection System (Bio-Rad) with the following conditions: 95°C for 15 min (1x); 95°C for 15 sec, 58°C for 30 sec, 72°C for 30 sec (45x); and 71 cycles of 60–95°C with a progressive increase of 0.5°C per cycle (melting). Each sample was analyzed in two technical duplicates.

Reaction efficiencies were analyzed using the LinRegPCR program (version 11.0), and the relative expression values were calculated by the Pfaffl method [54] using the REST software (Relative Expression Software Tool) [55]. The Pairwise Fixed Reallocation Randomization Test calculated the differential expression with 1000 bootstrap iterations, and the analyzed intervals were 6–0 h.a.i., 12–0 h.a.i. and 24–0 h.a.i.

Results

Mitochondrial genome of *A. psidii*

The mt genome assembly resulted in two contigs: 62,940 bp and 30,490 bp. By using CAP3 [56], the contigs were joined with a small overlapping region (approximately 70 bp), confirmed by PCR, resulting in a single contig of 93,299 bp (Fig 1). The *A. psidii* mitochondrial genome sequence presented a GC content of 37.39%, very similar to other published rust mtDNA.

Mitochondrial genome annotation

The MFannot predicted 73 different ORFs. Among them, the 14 mitochondrial core protein-coding genes were identified (Table 3). The results showed that 23 tRNA genes and all other 14 core genes transcribe from the same DNA strand clockwise (Fig 1). Details of *A. psidii* MF-1 core proteins were presented in S1 Table.

Besides, we identified 33 nonconserved ORFs (ncORFs). The ncORFs represent approximately 45% of the total genes found in this genome. We identified intronic ncORFs in 11 introns of conserved genes (one in the *cob*, one in the *cox2*, and 9 in the *cox1* genes). These

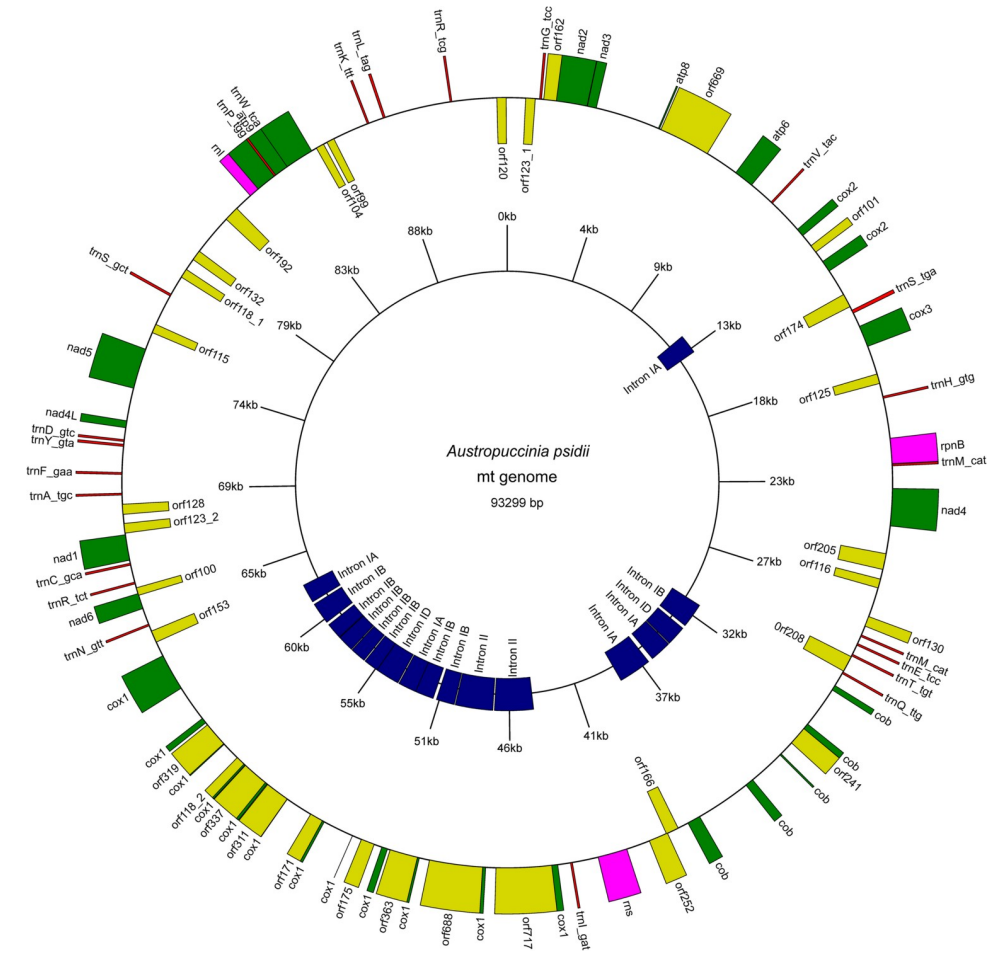


Fig 1. The mitochondrial genome of *Austropuccinia psidii* MF-1. The mitochondrial view was obtained by the Genome Vx tool (<http://wolfe.ucd.ie/GenomeVx/>).

<https://doi.org/10.1371/journal.pone.0248054.g001>

ncORFs encode for a ribosomal protein, LAGLIDADG endonucleases, and reverse transcriptases (RT) (Table 3). Some of the ncORFs have alternative start codons. In contrast to the conserved core genes, the ncORFs were found on both strands (S2 Table). In other rust mtDNA, only LAGLIDADG endonucleases were detected as HEG (S3 Table).

The mitochondrial genome was screened for codon usage, and the genes were analyzed for their start and stop codons (S1 and S2 Tables). Among the predicted genes, the 'AUG' was the initiation codon in all 14 conserved core genes. However, in ncORFs, the start codons 'UAU', 'GAA', 'AGU', 'UGA', 'CAA', 'GGU', 'GCC', and 'ACG' were found. The most frequent stop codon was 'UAA' (Fig 2).

Rust mtDNA comparative phylogenetic analysis

Among the six rust mtDNA evaluated, *A. psidii* had the largest number of genes and mtDNA size, followed by *Puccinia* spp. (77,600 bp on average). The *Phakospora* spp. had the smallest rust mitochondrial genome (32,172 bp on average). The GC content of *A. psidii* mtDNA did not differ from other rust mtDNAs. The *Phakospora* spp. mtDNA lacked the *rpnB* gene. The organization of core genes was conserved among the rust mitochondrial genomes (Fig 3A and

Table 3. Predicted genes of *Austropuccinia psidii* MF-1 mitochondrial genome.

Predicted genes	Encoded protein	Interesting features
Respiratory chain proteins		
Complex I		
<i>nad1</i>	NADH dehydrogenase subunit 1	contiguous and in phase with <i>orf162</i>
<i>nad2</i>	NADH dehydrogenase subunit 2	
<i>nad3</i>	NADH dehydrogenase subunit 3	
<i>nad4</i>	NADH dehydrogenase subunit 4	
<i>nad4L</i>	NADH dehydrogenase subunit 4L	
<i>nad5</i>	NADH- dehydrogenase subunit 5	
<i>nad6</i>	NADH- dehydrogenase subunit 6	
Complex III		
<i>cob</i>	Cytochrome b	4 introns I2—group = ID I3 and I4 -group = IA(5')
Complex IV		
<i>cox1</i>	Cytochrome c oxidase subunit 1	11 introns group II—I1 and I2 group = IA—I5 and I12 group = IB—I3, I4, I7, I8, I9, I10 and I11 group = ID—I6
<i>cox2</i>	Cytochrome c oxidase subunit 2	1 intron
<i>cox3</i>	Cytochrome c oxidase subunit 3	alternative ATG start pos 17117
Complex V		
<i>atp6</i>	ATP synthase subunit a	
<i>atp8</i>	ATP synthase subunit b	1 intron
<i>atp9</i>	ATP synthase subunit 9	alternative ATG start pos 85321
rRNA		
<i>Rns</i>	-	
<i>Rnl</i>	-	
Other proteins		
<i>rpnB</i>	recombination-promoting nuclease RpnB	
ncORFs		
<i>orf99</i>	hypothetical protein	Intergenic ncORF
<i>orf100</i>	hypothetical protein	Intergenic ncORF; in opposite strand of <i>nad6</i>
<i>orf101</i>	LAGLIDADG endonuclease	Intronic ncORF (<i>cox2</i> -I1)
<i>orf104</i>	hypothetical protein	Intergenic ncORF; in same sequence opposite strand of ATP9
<i>orf115</i>	hypothetical protein	Intergenic ncORF
<i>orf116</i>	hypothetical protein	Intergenic ncORF; TTG upstream: 27503
<i>orf118_1</i>	hypothetical protein	Intergenic ncORF
<i>orf118_2</i>	LAGLIDADG endonuclease	Intronic ncORF (<i>cox1</i> -I9) First aa- Tyr
<i>orf120</i>	hypothetical protein	Intergenic ncORF
<i>orf123_1</i>	hypothetical protein	Intergenic ncORF
<i>orf123_2</i>	hypothetical protein	Intergenic ncORF
<i>orf125</i>	hypothetical protein	Intergenic ncORF
<i>orf128</i>	hypothetical protein	Intergenic ncORF

(Continued)

Table 3. (Continued)

Predicted genes	Encoded protein	Interesting features
<i>orf130</i>	hypothetical protein	Intergenic ncORF
<i>orf132</i>	hypothetical protein	Intergenic ncORF
<i>orf153</i>	hypothetical protein	Intergenic ncORF; TTG upstream: 64208
<i>orf162</i>	hypothetical protein	<i>nad2</i> gene continuous and in phase with <i>orf162</i>
<i>orf166</i>	DEAD/DEAH box helicase domain	Intergenic ncORF
<i>orf171</i>	LAGLIDADG endonuclease	Intronic ncORF (<i>cox1</i> -I9); First aa- Glu;
<i>orf174</i>	hypothetical protein	Intergenic ncORF
<i>orf175</i>	LAGLIDADG endonuclease	Intronic ncORF (<i>cox1</i> -I4)
<i>orf192</i>	hypothetical protein	Intergenic ncORF
<i>orf205</i>	hypothetical protein	Intergenic ncORF; TTG upstream: 26703
<i>orf208</i>	hypothetical protein	Intergenic ncORF
<i>orf241</i>	LAGLIDADG endonuclease	Intronic ncORF (<i>cob</i> -I2) First aa-Ser
<i>orf252</i>	ribosomal protein S3	Intergenic ncORF
<i>orf311</i>	LAGLIDADG endonuclease	Intronic ncORF (<i>cox1</i> -I7); Codon alternative para UGA para Trp
<i>orf319</i>	LAGLIDADG endonuclease	Intronic ncORF (<i>cox1</i> -I10) First aa-Ile
<i>orf337</i>	LAGLIDADG endonuclease	Intronic ncORF (<i>cox1</i> -I8) First aa-Gln
<i>orf363</i>	LAGLIDADG endonuclease	Intronic ncORF (<i>cox1</i> -I3) First aa- Gly
<i>orf669</i>	reverse transcriptase	Intronic ncORF (<i>atp8</i> I1)
<i>orf688</i>	reverse transcriptase	Intronic ncORF (<i>cox1</i> -I2) First aa- Gly
<i>orf717</i>	reverse transcriptase	Intronic ncORF(<i>cox1</i> -I1) First aa- Thr

<https://doi.org/10.1371/journal.pone.0248054.t003>

3B). However, the total size of intronic and intergenic regions among them was highly variable. *A. psidii* has the largest amount of ncORF sequences (Fig 3C) and intronic sequences.

Genes *cox1* and *cob* presented introns in mtDNA of all rust pathogens (Table 4). Almost all of the introns detected in six of all the genes carried some HEG. The number of LAGLIDADG endonucleases encoded in intronic ncORF ranged from three in the soybean rust (*P. pachyrhizi*) to nine in *A. psidii*. Compared with other rust pathogens, *A. psidii* showed a higher

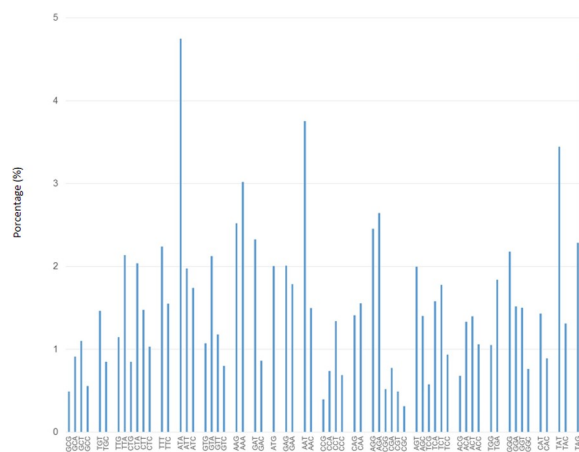


Fig 2. Column diagram of the *Austropuccinia psidii* mtDNA codon usage. The diagram represents the codons (x-axis) and percentages of their occurrence (y-axis) in the *A. psidii* mitochondrial genome.

<https://doi.org/10.1371/journal.pone.0248054.g002>

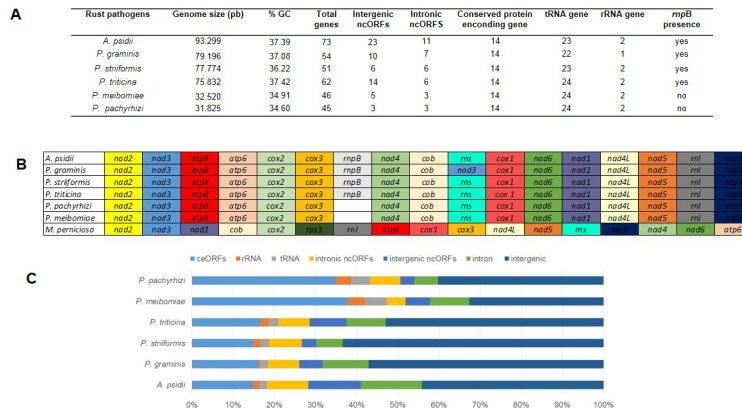


Fig 3. Comparison of the mitochondrial genome from *Austropuccinia psidii* and other rust. (A) General comparison of mitochondrial genome content among *A. psidii* and *P. graminis*, *P. striiformis*, *P. triticina*, *P. meibomia* and *P. pachyrhizi*, (B) Organization of core genes among the rust mitochondrial genomes, (C) Proportions of ceORFs, rRNA, tRNA, intronic and intergenic ncORFs, intron and intergenic content in the rust mitochondrial genomes.

<https://doi.org/10.1371/journal.pone.0248054.g003>

diversity of HEGs and intron groups: nine LAGLIDADG endonucleases, three reverse transcriptases, and six intron group IA, eight IB, two ID, and two II (S4 and S5 Tables).

Rust mtDNAs encode a similar number of tRNA genes. Only *A. psidii* has two tRNAs for glutamic acid (Glu) and a unique anticodon for lysine (Lys) (Table 5).

We compared the phylogeny using all 14 core proteins encoded by the mtDNA with the one of the *cox1*. The results showed that the multigene approach supported *A. psidii* as a sister clade to *Puccinia* spp. However, using *cox1*, the result was different, *A. psidii* clustered with *Phakospora* spp., although with low branch support (Fig 4A and 4B). The 18S rDNA-based phylogenetic analysis corroborated the clustering of *A. psidii* as a sister clade of *Puccinia* spp. (S1 Fig).

Proteomic and RT-qPCR analysis

Of the 33 ncORFs found in *A. psidii* mtDNA, we identified three of them in a previously generated proteomic dataset [14]: *orf174*, *orf205*, and *orf208*. Only *orf174* was present in other rust fungi, such as *P. graminis*. *Orf205* and *orf208* were unique to mtDNA of *A. psidii* (S6 Table). Using the software MOTIF, we found a conserved domain in *orf174*, identified as belonging to DNA topoisomerase I superfamily cl27598. *Orf205* has two conserved domains: one similar to the peroxidase family2 and another described as DUF2070. The *orf208* has the DUF2070 domain, as well (S7 Table).

We performed RT-qPCR analysis to confirm the expression of *orf174*, *orf205*, and *orf208* during fungal *in vitro* morphogenesis. Only the expression of *orf208* was detected. We

Table 4. Number of introns in conserved protein-coding genes in mtDNA of rust pathogens.

Rust pathogens	<i>atp8</i>	<i>cob</i>	<i>cox1</i>	<i>cox2</i>	<i>nad4</i>	<i>nad5</i>	Total
<i>A. psidii</i>	1	5	12	1			19
<i>P. meibomia</i>		1	4				5
<i>P. pachyrhizi</i>		1	4				5
<i>P. graminis</i>		2	5	1	1	2	11
<i>P. striiformis</i>		2	6	1	1	1	11
<i>P. triticina</i>		2	7	1		1	11

<https://doi.org/10.1371/journal.pone.0248054.t004>

Table 5. tRNAs present in the rust pathogens mtDNA.

Amino Acid	<i>P. meibomiae</i>	<i>P. pachyrhizi</i>	<i>P. graminis</i>	<i>P. striiformis</i>	<i>P. triticinia</i>	<i>A. psidii</i>
	Anticodon	Anticodon	Anticodon	Anticodon	Anticodon	Anticodon
Ala	TGC	TGC	TGC	TGC	TGC	TGC
Arg	TCG	TCG	TCG	TCG	TCG	TCG
	TCT	TCT	TCT	TCT	TCT	TCT
Asn	GTT	GTT	GTT	GTT	GTT	GTT
Asp	GTC	GTC	GTC	GTC	GTC	GTC
Cys	GCA	GCA	GCA	GCA	GCA	GCA
Gln	TTG	TTG	TTG	-	TTG	TTG
Glu	TTC	TTC	TTC	TTC	TTC	TTC
	-	-	-	-	-	TCC
Gly	TCC	TCC	TCC	TCC	TCC	-
His	GTG	GTG	GTG	GTG	GTG	GTG
Ile	GAT	GAT	-	GAT	GAT	GAT
Leu	TAG	TAG	TAG	TAG	TAG	TAG
Lys	TTT	TTT	TTT	TTT	TTT	TTT
	CTT	CTT	CTT	CTT	CTT	-
Met	CAT	CAT	CAT	CAT	CAT	CAT
	CAT	CAT	CAT	CAT	CAT	CAT
Phe	GAA	GAA	GAA	GAA	GAA	GAA
Pro	TGG	TGG	TGG	TGG	TGG	TGG
Ser	GCT	GCT	GCT	GCT	GCT	GCT
	TGA	TGA	TGA	TGA	TGA	TGA
Sup	TCA	TCA	TCA	TCA	TCA	TCA
Thr	TGT	TGT	TGT	TGT	TGT	TGT
Tyr	GTA	GTA	-	GTA	GTA	GTA
Val	TAC	TAC	TAC	TAC	TAC	TAC
	24	24	22	23	24	23

<https://doi.org/10.1371/journal.pone.0248054.t005>

observed a gradual downregulation of the expression during the development of germinative tubes and appressorium formation (Fig 5).

Discussion

Compared with other mtDNAs rust pathogens used in the present study, *A. psidii* had one of the largest ones. Fungal mitochondrial genomes are highly variable in size, ranging from 12 kb in the mycoparasite *Rozella allomyces* [57] to 235.8 kb of the fungus *Rhizoctonia solani* [58]. The mtDNA size variability may occur among organisms from the same species. The mtDNA from *P. striiformis* f. sp. *tritici* ranged 102,521 [59], approximately 25% bigger than the mtDNA from *P. striiformis* PST-78, used in the present study. Several factors contribute to size variations, including the proliferation of noncoding sequences such as short tandem repeats, gene duplication followed by inactivation, intron expansion, and incorporation of foreign sequences from different sources [25,58,60]. According to Medina *et al.* [25], within Dikarya in general, Basidiomycetes mtDNA is highly variable in gene order compared to Ascomycetes. Furthermore, while in Basidiomycetes, mtDNAs have genes usually encoded on both strands, in Ascomycetes, they are encoded in only one. Interestingly in *A. psidii* and other evaluated rust mtDNAs, the core genes are in the same strand.

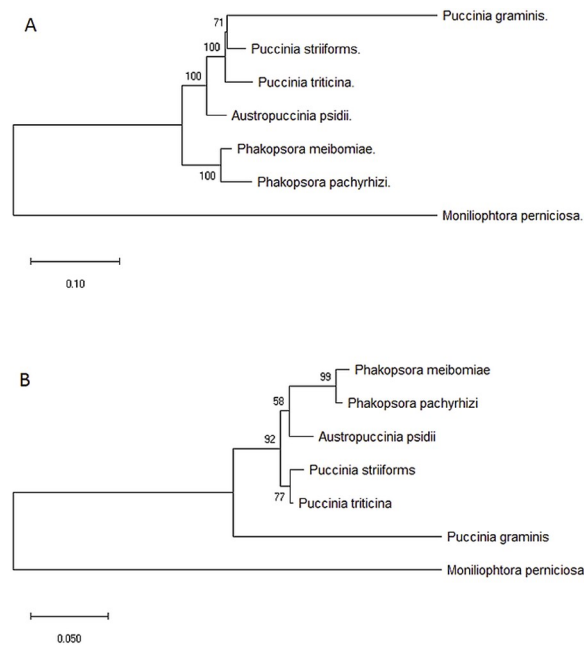


Fig 4. Maximum likelihood phylogenetic tree of rust mtDNA. The phylogeny analyses were based on the whole genome (A) and *cox1* (B) sequences. The sequences were aligned using the MUSCLE The statistical method Maximum Likelihood (bootstrap test with 1000 repetitions) and the Hasegawa—Kishino—Yano model were used for the phylogenetic tree construction. The numbers above tree nodes represent the bootstrap support values. *M. perniciosa* was used as an out-group.

<https://doi.org/10.1371/journal.pone.0248054.g004>

The large size of *A. psidii* mtDNA is partially associated with the abundance of ncORF. ncORFs are frequently reported in fungal mitochondrial genomes [61–65], but their origin and function are still unknown. For instance, the variable sizes of the mitochondrial genomes

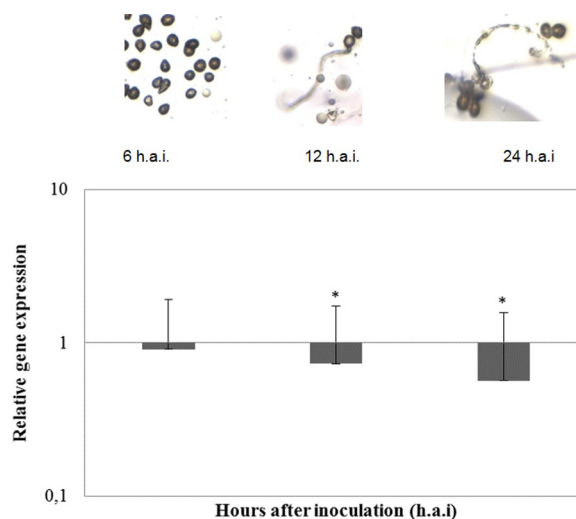


Fig 5. RT-qPCR analysis of *orf208* gene. Expression analysis of *orf208* from *A. psidii* MF-1 in three different times of *in vitro* fungal development. Expression values were normalized with beta-tubulin and elongation factor as a housekeeping reference Pfaffl [54]. Values represent the expression ratio of the *orf208* gene. Bars represent the mean for three replicates, and error bars show the standard error of the mean. Asterisks indicate values that differ significantly ($P_{0.05}$) between 0 and 6, 12 or 24 h after inoculation as determined by the method of Pfaffl et al. [55].

<https://doi.org/10.1371/journal.pone.0248054.g005>

of *Colletotrichum* species are due, in part, to the presence or absence of ncORFs and intronic sequences [66]. The large mtDNA size of *Phlebia radiata* (156 kbp) also harbors a large number of introns and long intergenic regions [63].

A. psidii had the largest number of ncORFs in intronic regions among the mtDNAs assessed in this work. Many of the ncORFs were related to HEGs, primarily LAGLIDADG endonucleases. Queiroz *et al.* [66] observed that *C. lindemuthianum* contains just one intronic ncORF encoding a LAGLIDADG endonuclease. However, more than one intronic ncORF encoding LAGLIDADG endonucleases were found in rust mtDNA. HEGs can expand mtDNA size, cause genome rearrangements, gene duplications, and import exogenous nucleotide sequences through horizontal gene transfer (HGT) [67,68]. HEGs may also be involved in the spread of group I introns between distant species [69,70].

Concerning the HEGs found in rust mtDNA, we identified only LAGLIDADG encoding genes. These sequences are self-splicing and play relevant roles in processes associated with genome evolution [71]. Many group I intron-encoded LAGLIDADG proteins function as maturases assisting in RNA splicing [72–75]. This activity described in fungi such as *Saccharomyces cerevisiae*, *Saccharomyces capensis*, *Aspergillus nidulans* [73,75,76], suggests that endonuclease and maturase activities are close in function and evolution to LAGLIDADG proteins encoded by group-I introns in rust fungi [77]. GIY-YIG ORFs have been reported in introns of fungal mitochondria [77,78]. However, no GIY-YIG endonucleases were found in rust mtDNA.

Mobile elements, including HEGs, play a crucial role in the expansion of fungal mitochondrial genomes. We observed a relationship between the genome size and total mobile elements hosted in intronic sequences in rust fungi. The number of introns is highly variable among mitochondrial genomes; for example, *Fusarium graminearum* has 34 group-I introns [79], whereas *Mycosphaerella graminicola* has no introns [80]. Ambrosio *et al.* [81] revealed that 48.7% of *C. cacaofunesta* mtDNA was composed of introns. The number of intron groups in rust fungi mtDNA ranged between 3–18 to *P. meibomiae* and *A. psidii*, respectively. There is a lack of available complete mtDNA sequence of Pucciniales. Thus, our research may bring a significant contribution to the comprehension and phylogeny of this group. In our studies using mtDNA from Pucciniales, phylogenetic analyses revealed that according to core genes, *A. psidii* was confidently a sister clade of *Puccinia* spp. This result is in agreement with the 18S rDNA phylogenetic analysis. Similarly, Zhang *et al.* [82] observed a congruency between nuclear ribosomal RNA and mitochondrial protein-based trees to *Cordyceps militaris*. Our phylogeny data demonstrated that mitochondrial core genes are an alternative for determining phylogenetic relationships among rust fungi, as shown in other species of fungi and other organisms [83–85].

We need broader taxon sampling to include all the phylogenetic diversity of the group and achieve a robust phylogeny and evolutionary trajectory, including the mobile element. The mobile genetic elements and features such as the number of introns per gene and similar positions were more similar between *A. psidii*–*Puccinia* spp. than that of *A. psidii*–*Phakopsora*.

Interestingly, comparing only *cox1* from complete mtDNA of the six Pucciniales, *A. psidii* was closer to *Phakopsora* spp, although with notably low branch support. This data supports the fact that since the degree of conservation and organization of genes may vary according to the group studied, a preliminary analysis is essential to select "a priori" reliable phylogenetic markers [25]. Mitochondrial genes, such as *cox1*, were widely used for barcoding many groups of organisms, although with less identification power in the fungal kingdom due to the rapid evolution of their mt genomes [27]. Wang *et al.* [86] demonstrated that the frequent heteroplasmy and recombination in the mitochondrial genomes of *Thelephora ganbajun* resulted in two types of introns in different sites of *cox1* with varying frequencies among the isolates.

Allelic association analyses of the observed mitochondrial polymorphic nucleotide in *cox1* sites suggested that mtDNA recombination is frequent in natural populations of this fungus. Li *et al.* [87] assembled the mtDNAs of *Pleurotus citrinopileatus* and *Pleurotus platypus* and observed thirteen classes of introns (Pcls) within the *cox1* gene. The number and class of Pcls varied among different *Pleurotus* species, indicating that the introns in *cox1* directed the mitochondrial genome rearrangements. Only concatenated mitochondrial protein sequences were suitable as molecular markers for phylogenetic analysis of *Pleurotus* spp.

We identified three out of the 33 ncORFs in our previous proteomic datasets [14]. The only conserved region of these proteins was the DUF2070 domains, with TM-regions found in *orf208* and *orf205*. According to Tang *et al.* [88], the mitochondrial membrane protein FgLetm1, containing DUF2070, regulates mitochondrial integrity, production of endogenous reactive oxygen species and mycotoxin biosynthesis in *Fusarium graminearum*. The authors obtained Δ FgLetm1 mutant that significantly reduced endogenous ROS levels, decreased mycotoxin deoxynivalenol biosynthesis, and attenuated virulence *in planta*. Thus, we suggest that *orf208* and *orf205* encode a transmembrane protein that may be related to fungal pathogenicity. According to the RT-qPCR results, the only transcribed gene was *orf208*. The gene was down-regulated during the fungal morphogenesis.

Nine of the 33 ncORFs identified in the *A. psidii* mtDNA presented alternative start codons. We strongly believe that they are not pseudogenes. It is known that mtDNA and other plastid genomes are composed of a significant number of genes with alternative codons, most of them related with mobile elements [89,90]. The nine ncORFs (*orf118_2*, *orf171*, *orf241*, *orf311*, *orf319*, *orf337*, *orf363*, *orf688*, *orf717*) with alternative start codons were associated with mobile elements that may be related to the evolution of the mtDNA in progress [77,91]. More assays using different stimuli and assays carried out *in planta* should be performed to validate the ncORFs presence encoding protein to help understand the function of these ncORFs in mtDNA *A. psidii*. We also showed the first experimental evidence of three new mitochondrial proteins exclusive of *A. psidii*. Furthermore, the functional characterization of these proteins and their association with particular mitochondrial pathways or during host interaction is a valuable tool to elucidate important biological features of myrtle rust disease.

Supporting information

S1 Fig. Maximum likelihood phylogenetic tree of rust pathogens based on 18S rDNA partial sequences obtained from the GenBank nucleotide sequence database. The accession numbers are in parentheses. The sequences were aligned using the MUSCLE method. For the phylogenetic tree construction, the statistical methods Maximum Likelihood, the Bootstrap method test with 1000 repetitions, and the Hasegawa—Kishino—Yano model were performed. The numbers above tree nodes represent the bootstrap support values. *M. pernicioso* was used as an out-group.

(DOCX)

S1 Table. Conserved gene features of the *Austropuccinia psidii* MF-1 mitochondrial genome.

(DOCX)

S2 Table. Nonconserved ORFs (ncORFs) features of the *Austropuccinia psidii* MF-1 mitochondrial genome.

(DOCX)

S3 Table. Nonconserved ORFs (ncORFs) features in mtDNA rust pathogens.

(DOCX)

S4 Table. Number of LAGLIDADG endonucleases and intron types present in introns of six genes gene in mtDNA of rust pathogens.

(DOCX)

S5 Table. Features of introns characterized in mtDNA of rust pathogens.

(DOCX)

S6 Table. Nonconserved ORFs (ncORFs) in mtDNA *Austropuccinia psidii* MF-1 shared by other rust pathogens.

(DOCX)

S7 Table. Conserved domain in unknown function proteins found in *Austropuccinia psidii*.

(DOCX)

Acknowledgments

We thank Dr. Thais Regiani for supporting the proteomic analysis. We are grateful for the efforts of Dr. Andressa Peres Bini in developing the previous RT-qPCR protocol analyses.

Author Contributions

Conceptualization: Jaqueline Raquel de Almeida, Diego Mauricio Riaño Pachón, Claudia Barros Monteiro-Vitorello, Maria Carolina Quecine.

Data curation: Jaqueline Raquel de Almeida, Diego Mauricio Riaño Pachón, Livia Maria Franceschini, Pedro Avelino Maia de Andrade.

Formal analysis: Livia Maria Franceschini, Isaneli Batista dos Santos, Pedro Avelino Maia de Andrade.

Funding acquisition: Carlos Alberto Labate, Maria Carolina Quecine.

Investigation: Jaqueline Raquel de Almeida, Diego Mauricio Riaño Pachón, Isaneli Batista dos Santos, Jessica Aparecida Ferrarezi, Pedro Avelino Maia de Andrade, Maria Carolina Quecine.

Methodology: Jaqueline Raquel de Almeida, Diego Mauricio Riaño Pachón, Livia Maria Franceschini, Isaneli Batista dos Santos, Jessica Aparecida Ferrarezi, Pedro Avelino Maia de Andrade, Maria Carolina Quecine.

Resources: Maria Carolina Quecine.

Software: Diego Mauricio Riaño Pachón, Livia Maria Franceschini, Pedro Avelino Maia de Andrade.

Supervision: Maria Carolina Quecine.

Writing – original draft: Jaqueline Raquel de Almeida, Maria Carolina Quecine.

Writing – review & editing: Jaqueline Raquel de Almeida, Diego Mauricio Riaño Pachón, Livia Maria Franceschini, Isaneli Batista dos Santos, Jessica Aparecida Ferrarezi, Pedro Avelino Maia de Andrade, Claudia Barros Monteiro-Vitorello, Carlos Alberto Labate, Maria Carolina Quecine.

References

1. Dean R, Van Kan JAL, Pretorius ZA, Hammond-Kosack KE, Di Pietro A, Spanu PD et al. The top 10 fungal pathogens in molecular plant pathology. *Mol. Plant Pathol.* 2012; 13,414–430. <https://doi.org/10.1111/j.1364-3703.2011.00783.x> PMID: 22471698
2. Winter G. Repertorium. Rabenhorstii fungi europaei et extraeuropaeei. Centuria XXXI et XXXII. 1884. *Hedwigia*, 23, 164–175.
3. Beenken L. *Austropuccinia*: a new genus name for the myrtle rust *Puccinia psidii* placed within the redefined family Sphaerophragmiaceae (Pucciniales). *Phytotaxa*. 2017; 297 (1), 53–61. <https://doi.org/10.11646/phytotaxa.297.1.5>
4. Dodds PN, Rafiqi M, Gan PHP, Hardham AR, Jones DA, Ellis JG. Effectors of biotrophic fungi and oomycetes: pathogenicity factors and triggers of host resistance. *New Phytol.* 2009; 183, 993–1000. <https://doi.org/10.1111/j.1469-8137.2009.02922.x> PMID: 19558422
5. Graça RN, Ross-Davis AL, Klopfenstein NB, Kim MS, Peever TL, Cannon PG et al. Rust disease of eucalypts, caused by *Puccinia psidii*, did not originate via host jump from guava in Brazil. *Mol. Ecol.* 2013; 22,6033e6047. <https://doi.org/10.1111/mec.12545> PMID: 24112757
6. Junghans DT, Alfenas AC, Brommonschenkel SH, Oda S, Mello EJ, Grattapaglia D. Resistance to rust (*Puccinia psidii* Winter) in *Eucalyptus*: mode of inheritance and mapping of a major gene with RAPD markers. *Theor. Appl. Genet.* 2003; 108: 175e180. <https://doi.org/10.1007/s00122-003-1415-9> PMID: 14504745
7. Machado PD, Glen M, Pereira OL, Silva AA, Alfenas AC. Epitypification of *Puccinia psidii*, causal agent of guava rust. *Trop. Plant Pathol.* 2015; 40, 5–12. <https://doi.org/10.1007/s40858-014-0002-8>
8. Quecine MC, Bini AP, Romagnoli EM, Andreote FD, Moon DH, Labate CA. Genetic variability of *Puccinia psidii* populations revealed by PCR-DGGE and T-RFLP markers. *Plant Dis.* 2014; 98, 16–23. <https://doi.org/10.1094/PDIS-03-13-0332-RE> PMID: 30708618
9. Makinson RO. Myrtle Rust reviewed: The impacts of the invasive plant pathogen *Austropuccinia psidii* on the Australian environment. Plant Biosecurity Cooperative Research Centre, Canberra. 2018 [Cited 13 August 2020]. Available from: <http://www.apbsf.org.au/wp-content/uploads/2018/11/Myrtle-Rust-reviewed-June-22-2018-web.pdf>.
10. Tan MK, Collins D, Chen Z, Englezou A, Wilkins MR. A brief overview of the size and composition of the myrtle rust genome and its taxonomic status. *Mycol.* 2014;5,2, 52–63. <https://doi.org/10.1080/21501203.2014.919967> PMID: 24999437
11. Sandhu KS, Karaoglu H, Zhang P, Park RF. Simple sequence repeat markers support the presence of a single genotype of *Puccinia psidii* in Australia. *Plant Pathology*. 2015; 65(7), 1084–1094. <https://doi.org/10.1111/ppa.12501>
12. McTaggart AR, Shuey LS, Granados GM, du Plessis E, Fraser S, Barnes I et al. Evidence that *Austropuccinia psidii* may complete its sexual life cycle on Myrtaceae. *Plant Pathol.* 2017; 67(3), 729–734. <https://doi.org/10.1111/ppa.12763>
13. Tobias PA, Schwessinger B, Deng CH, Wu C, Dong C, Sperschneider J et al. *Austropuccinia psidii*, causing myrtle rust, has a gigabase-sized genome shaped by transposable elements. *BioRxiv*. 2020.03.18.996108; <https://doi.org/10.1101/2020.03.18.996108>
14. Quecine MC, Leite TF, Bini AP, Regiani T, Franceschini LM, Budzinski IGF et al. Label free quantitative proteomic analysis of *Puccinia psidii* uredospores reveals differences of fungal populations infecting eucalyptus and guava. *PlosOne*. 2016; 11, p.e0145343. <https://doi.org/10.1371/journal.pone.0145343> PMID: 26731728
15. Santos IB, Lopes MS, Bini AP, Tschoeke BAP, Verssani BAW, Figueredo EF et al. The *Eucalyptus* Cuticular Waxes Contribute in Prefomed Defense Against *Austropuccinia psidii*. *Front. Plant Sci.* 2019; 9:1978. <https://doi.org/10.3389/fpls.2018.01978> PMID: 30687371
16. McTaggart AR, du Plessis E, Roux J, Barnes I, Fraser S, Granados GM et al. Sexual reproduction in populations of *Austropuccinia psidii*. *Eur J Plant Pathol.* 2020; 156:537–545. <https://doi.org/10.1007/s10658-019-01903-y>
17. Bullerwell CE, Lang BF. Fungal evolution: the case of the vanishing mitochondrion. *Curr. Opin. Microbiol.* 2005; 8(4), 362–369. <https://doi.org/10.1016/j.mib.2005.06.009> PMID: 15993645
18. Borriello R, Bianciotto V, Orgiazzi A, Lumini E, Bergero R. Sequencing and comparison of the mitochondrial COI gene from isolates of Arbuscular Mycorrhizal Fungi belonging to Gigasporaceae and Glomeraceae families. *Mol. Phylogenet. Evol.* 2014; 75(1), 1–10. <https://doi.org/10.1016/j.ympev.2014.02.012> PMID: 24569015
19. Lambowitz AM, Belfort M. Mobile bacterial group II introns at the crux of eukaryotic evolution. *Microbiol. Spectr.* 2015; 3(1), MDNA3-0050-2014. <https://doi.org/10.1128/microbiolspec.MDNA3-0050-2014> PMID: 26104554

20. Hurst GDD, Werren JH. The role of selfish genetic elements in eukaryotic evolution. *Nat. Rev. Genet.* 2001; 2(8), 597–606. <https://doi.org/10.1038/35084545> PMID: 11483984
21. Lang BF, Laforest MJ, Burger G. Mitochondrial introns: a critical view. *Trends Genet.* 2007; 23(3), 119–125. <https://doi.org/10.1016/j.tig.2007.01.006> PMID: 17280737
22. Wu B, Hao W. Horizontal transfer and gene conversion as an important driving force in shaping the landscape of mitochondrial introns. *G3/ Genes|Genomes|Genet.* 2014; 4(4), 605–612. <https://doi.org/10.1534/g3.113.009910> PMID: 24515269
23. Kolesnikova AI, Putintseva YA, Simonov EP, Biriukov VV, Oreshkova NV, Pavlov IN et al. Mobile genetic elements explain size variation in the mitochondrial genomes of four closely-related *Armillaria* species. *BMC Genomics.* 2019; 20, 351. <https://doi.org/10.1186/s12864-019-5732-z> PMID: 31068137
24. Ballard JWO, Whitlock MC. The incomplete natural history of mitochondria. *Mol. Ecol.* 13, 729–744. *Mol. Ecol.* 2004;13, 729–44. <https://doi.org/10.1046/j.1365-294x.2003.02063.x> PMID: 15012752
25. Medina R, Franco MEE, Bartel LC, Alcántara VM, Saparrat MCN, Balatti PA. Fungal mitogenomes: relevant features to planning plant disease management. *Front. Microbiol.* 2020; 11:978. <https://doi.org/10.3389/fmicb.2020.00978> PMID: 32547508
26. Song N, Geng Y, Li X. The mitochondrial genome of the phytopathogenic fungus *Bipolaris sorokiniana* and the utility of mitochondrial genome to infer phylogeny of Dothideomycetes. *Front. Microbiol.* 2020; 11:863. <https://doi.org/10.3389/fmicb.2020.00863> PMID: 32457727
27. Nadimi M, Daubois L, Hijri M. Mitochondrial comparative genomics and phylogenetic signal assessment of mtDNA among arbuscular mycorrhizal fungi. *Mol. Phylogenet. Evol.* 2016; 98, 74–83. <https://doi.org/10.1016/j.ympev.2016.01.009> PMID: 26868331
28. Pantou MP, Kouvelis VN, Typas MA. The complete mitochondrial genome of *Fusarium oxysporum*: insights into fungal mitochondrial evolution. *Gene.* 2008; 419, 7–15. <https://doi.org/10.1016/j.gene.2008.04.009> PMID: 18538510
29. Kim JO, Choi KY, Han JH, Choi I-Y, Lee YH, Kim KS. The complete mitochondrial genome sequence of the ascomycete plant pathogen *Colletotrichum acutatum*. *Mitochondrial DNA A DNA Mapp. Seq. Anal.* 2015; 1736, 1–2. <https://doi.org/10.3109/19401736.2015.1101556> PMID: 26539901
30. Jiménez-Becerril MF, Hernández-Delgado S, Solís-Oba M, González Prieto JM. Analysis of mitochondrial genetic diversity of *Ustilago maydis* in Mexico. *Mitochondrial DNA A DNA Mapp. Seq. Anal.* 2016; 29(1):1–8. <https://doi.org/10.1080/24701394.2016.1229776> PMID: 27728988
31. Aliyu SR, Lin L, Chen X, Abdul W, Lin Y, Otieno FJ et al. Disruption of putative short-chain acyl CoA dehydrogenases compromised free radical scavenging, conidiogenesis, and pathogenesis of *Magnaporthe oryzae*. *Fungal Genetics and Biology.* 2019; 127,23–34. <https://doi.org/10.1016/j.fgb.2019.02.010> PMID: 30822500
32. Bartelli TF, Bruno DCF, Briones MRS. Evidence for mitochondrial genome methylation in the yeast *Candida albicans*: a potential novel epigenetic mechanism affecting adaptation and pathogenicity? *Front. Genet.* 2018; 29:9,166. <https://doi.org/10.3389/fgene.2018.00166> PMID: 29896215
33. Chang AL, Doering TL. Maintenance of mitochondrial morphology in *Cryptococcus neoformans* is critical for stress resistance and virulence. *MBio.* 2018;6; 9(6). pii e01375–18. <https://doi.org/10.1128/mBio.01375-18> PMID: 30401774
34. Kretschmer M, Lambie S, Croll D, Kronstad JW. Acetate provokes mitochondrial stress and cell death in *Ustilago maydis*. *Mol. Microbiol.* 2017; 107, 488–507. <https://doi.org/10.1111/mmi.13894> PMID: 29235175
35. Leite TF, Moon DH, Lima ACM, Labate CA, Tanaka FAO. A simple protocol for whole leaf preparation to investigate the interaction between *Puccinia psidii* and *Eucalyptus grandis*. *Australas. Plant Pathol.* 2013; 42, 79–84. <https://doi.org/10.1007/s13313-012-0179-6>
36. Hahn C, Bachmann L, Chevreux B. Reconstructing mitochondrial genomes directly from genomic next-generation sequencing reads—a baiting and iterative mapping approach, *Nucleic Acids Res.* 2013; 41 (13), e129. <https://doi.org/10.1093/nar/gkt371> PMID: 23661685
37. Chaisson MJ, Glenn T. Mapping single molecule sequencing reads using basic local alignment with successive refinement (BLASR): application and theory. *BMC Bioinformatics.* 2012; 13, 238. <https://doi.org/10.1186/1471-2105-13-238> PMID: 22988817
38. Bankevich A, Nurk S, Antipov D, Gurevich AA, Dvorkin M, Kulikov AS et al. SPAdes: a new genome assembly algorithm and its applications to single-cell sequencing. *J. Comput.* 2012; 19(5), 455–477. <https://doi.org/10.1089/cmb.2012.0021> PMID: 22506599
39. Gurevich A, Saveliev V, Vyahhi N, Tesler G. QUAST: quality assessment tool for genome assemblies. *Bioinform.* 2013; 29(8), 1072–1075. <https://doi.org/10.1093/bioinformatics/btt086> PMID: 23422339
40. Hasegawa M, Kishino H, Yano T. Dating of the human-ape splitting by a molecular clock of mitochondrial DNA. *J. Mol. Evol.* 1985; 22, 160–174. <https://doi.org/10.1007/BF02101694> PMID: 3934395

41. Beck N, Lang BF. Mfannot. 2010 [cited 25 March 2019] Available from: <http://megasun.bch.umontreal.ca/cgi-bin/mfannot/mfannotInterface.pl>.
42. Tillich M, Lehwark P, Pellizzer T, Ulbricht-Jones ES, Fischer A, Bock R, et al. GeSeq—versatile and accurate annotation of organelle genomes. *Nucl. Acids Res.* 2017; 45: W6–W11. <https://doi.org/10.1093/nar/gkx391> PMID: 28486635
43. Lowe TM, Eddy SR. tRNAscan-SE: a program for improved detection of transfer RNA genes in genomic sequence. *Nucl. Acids Res.* 1997; 25:955–964. <https://doi.org/10.1093/nar/25.5.955> PMID: 9023104
44. Formighieri EF, Tiburcio RA, Armas ED, Medrano FJ, Shimo H, Carels N et al. The mitochondrial genome of the phytopathogenic basidiomycete *Moniliophthora perniciosa* is 109 kb in size and contains a stable integrated plasmid. *Mycol. Res.* 2008; 112, 1136–1152. <https://doi.org/10.1016/j.mycres.2008.04.014> PMID: 18786820
45. Kumar S, Stecher G, Tamura K. MEGA7: molecular evolutionary genetics analysis version 7.0 for bigger datasets. *Mol. Biol. Evol.* 2016; 33(7), 1870–1874. <https://doi.org/10.1093/molbev/msw054> PMID: 27004904
46. Capella-Gutierrez S, Silla-Martinez JM, Gabaldon T. trimAl: a tool for automated alignment trimming in large-scale phylogenetic analyses. *Bioinformatics.* 2009; 25,1972–1973. <https://doi.org/10.1093/bioinformatics/btp348> PMID: 19505945
47. Nylander JAA. MrModeltest v2. Program distributed by the author. Evolutionary Biology Centre, Uppsala University. 2004.
48. Maddison WP, Maddison DR. Mesquite: a modular system for evolutionary analysis. Version 3.51. 2018 [cited 4 April 2019]. Available from: <http://www.mesquiteproject.org>.
49. Edgar RC. MUSCLE: multiple sequence alignment with high accuracy and high throughput. *Nucleic Acids Res.* 2004; 32, 1792–179. <https://doi.org/10.1093/nar/gkh340> PMID: 15034147
50. Silva JC, Gorenstein MV, Li G-Z, Vissers JPC, Geromanos SJ. Absolute quantification of proteins by LCMSE: a virtue of parallel MS acquisition. *Mol Cell Proteomics.* 2006; 5(1):144–56. <https://doi.org/10.1074/mcp.M500230-MCP200> PMID: 16219938
51. Bini AB, Quecine MQ, da Silva TM, Silva LD, Labate CA. Development of a quantitative real-time PCR assay using SYBR Green for early detection and quantification of *Austropuccinia psidii* in *Eucalyptus grandis*. *Euro. J. Plant Pathol.* 2018; 150,735–746. <https://doi.org/10.1007/s10658-017-1321-7>
52. Bini AP. Estudo molecular do desenvolvimento de *Puccinia psidii* Winter in vitro e no processo de infecção em *Eucalyptus grandis*. PhD thesis, Escola Superior de Agricultura Luiz de Queiroz, Brazil. 2016. Available from: <https://teses.usp.br/teses/disponiveis/11/11137/tde-10112016-161846/pt-br.php>.
53. Lopes MS. Identificação in silico e perfil transcricional de genes candidatos a efetores de *Austropuccinia psidii*. Master's dissertation, Escola Superior de Agricultura "Luiz de Queiroz"/USP, Brazil. 2017. Available from: <https://teses.usp.br/teses/disponiveis/11/11137/tde-22032018-145215/pt-br.php>.
54. Pfaffl MW. A new mathematical model for relative quantification in real-time RT-PCR. *Nucl. Acids Res.* 2001; 29:e45. <https://doi.org/10.1093/nar/29.9.e45> PMID: 11328886
55. Pfaffl MW, Horgan GW, Dempfle L. Relative expression software tool (REST©) for group-wise comparison and statistical analysis of relative expression results in real-time PCR. *Nucl. Acids Res.* 2002; 30: e36. <https://doi.org/10.1093/nar/30.9.e36> PMID: 11972351
56. Huang X, Madan A. CAP3: A DNA sequence assembly program. *Genome Res.* 1999; 9, 868–877. <https://doi.org/10.1101/gr.9.9.868> PMID: 10508846
57. James TY, Pelin A, Bonen L, Ahrendt S, Sain D, Corradi N, et al. Shared signatures of parasitism and phylogenomics unite Cryptomycota and microsporidia. *Curr. Biol.* 2013; 23(16), 1548–1553. <https://doi.org/10.1016/j.cub.2013.06.057> PMID: 23932404
58. Losada L, Pakala SB, Fedorova ND, Joardar V, Shabalina SA, Hostetler J et al. Mobile elements and mitochondrial genome expansion in the soil fungus and potato pathogen *Rhizoctonia solani* AG-3. *FEMS Microbiol. Lett.* 2014; 352(2), 165–173. <https://doi.org/10.1111/1574-6968.12387> PMID: 24461055
59. Li C, Lu X, Zhang Y, Liu Na, Li C, Zheng W. The complete mitochondrial genomes of *Puccinia striiformis* f. sp. *tritici* and *Puccinia recondita* f. sp. *tritici*, Mitochondrial DNA B. 2020. 5(1), 29–30. <https://doi.org/10.1080/23802359.2019.1674744> PMID: 33366407
60. Burger G, Gray MW, Lang BF. Mitochondrial genomes: anything goes. *Trends Genet.* 2003; 19(12), 709–716. <https://doi.org/10.1016/j.tig.2003.10.012> PMID: 14642752
61. Jelen V, De Jonge R, Van De Peer Y, Javornik B, Jakše J. Complete mitochondrial genome of the Verticillium-wilt causing plant pathogen *Verticillium nonalfalfae*. *PLoS One.* 2016; 11(2), e0148525. <https://doi.org/10.1371/journal.pone.0148525> PMID: 26839950
62. Li Y, Hu XD, Yang RH, Hsiang T, Wang K, Liang DQ et al. Complete mitochondrial genome of the medicinal fungus *Ophiocordyceps sinensis*. *Sci. Rep.* 2015; 5(1),13892. <https://doi.org/10.1038/srep13892> PMID: 26370521

63. Salavirta H, Oksanen I, Kuuskeri J, Mäkelä M, Laine P, Paulin L, et al. Mitochondrial genome of *Phlebia radiata* is the second largest (156 kbp) among fungi and features signs of genome flexibility and recent recombination events. *PLoS One*. 2014; 9(5),e97141. <https://doi.org/10.1371/journal.pone.0097141> PMID: 24824642
64. Torriani SFF, Penselin D, Knogge W, Felder M, Taudien S, Platzer M et al. Comparative analysis of mitochondrial genomes from closely related *Rhynchosporium* species reveals extensive intron invasion. *Fungal Genet. Biol.* 2014; 62, 34–42. <https://doi.org/10.1016/j.fgb.2013.11.001> PMID: 24240058
65. Zhang S, Wang X-N, Zhang X-L, Liu X-Z, Zhang Y-J. Complete mitochondrial genome of the endophytic fungus *Pestalotiopsis fici*: features and evolution. *Appl. Microbiol. Biotechnol.* 2017; 101(4):1593–1604. <https://doi.org/10.1007/s00253-017-8112-0> PMID: 28097404
66. Queiroz CB, Santana MF, Vidigal PMP, Queiroz MV. Comparative analysis of the mitochondrial genome of the fungus *Colletotrichum lindemuthianum*, the causal agent of anthracnose in common beans. *Appl. Microbiol. Biotechnol.* 2018; 102, 2763–2778. <https://doi.org/10.1007/s00253-018-8812-0> PMID: 29453633
67. Beaudet D, Nadimi M, Iffis B, Hijri M. Rapid mitochondrial genome evolution through invasion of mobile elements in two closely related species of arbuscular mycorrhizal fungi. *PLoS One*. 2013; 8(4), e60768. <https://doi.org/10.1371/journal.pone.0060768> PMID: 23637766
68. Joardar V, Abrams NF, Hostetler J, Paukstelis PJ, Pakala S, Pakala SB et al. Sequencing of mitochondrial genomes of nine *Aspergillus* and *Penicillium* species identifies mobile introns and accessory genes as main sources of genome size variability. *BMC Genomics*. 2012; 13(1), 698. <https://doi.org/10.1186/1471-2164-13-698> PMID: 23234273
69. Gonzalez P, Barroso G, Labarère J. Molecular analysis of the split *cox1* gene from the Basidiomycota *Agrocybe aegerita*: relationship of its introns with homologous Ascomycota introns and divergence levels from common ancestral copies. *Gene*. 1998; 220, 45–53. [https://doi.org/10.1016/s0378-1119\(98\)00421-1](https://doi.org/10.1016/s0378-1119(98)00421-1) PMID: 9767103
70. Vaughn JC, Mason MT, Sper-Whitis GL, Kuhlman P, Palmer JD. Fungal origin by horizontal transfer of a plant mitochondrial group I intron in the chimeric *coxI* gene of *Peperomia*. *J Mol Evol.* 1995; 41 (5):563–72. 36. <https://doi.org/10.1007/BF00175814> PMID: 7490770
71. Schuster A, Lopez JV, Becking LE, Kelly M, Pomponi SA, Wörheide G et al. Evolution of group I introns in Porifera: new evidence for intron mobility and implications for DNA barcoding. *BMC Evol Biol.* 2017; 17:82. <https://doi.org/10.1186/s12862-017-0928-9> PMID: 28320321
72. Chi SI, Dahl M, Emblem Å, Johansen SD. Giant group I intron in a mitochondrial genome is removed by RNA back-splicing. *BMC Mol Biol.* 2019 20(1), 16. <https://doi.org/10.1186/s12867-019-0134-y> PMID: 31153363
73. Ho Y, Kim SJ, Waring RB. A protein encoded by a group I intron in *Aspergillus nidulans* directly assists RNA splicing and is a DNA endonuclease. *Proc Natl Acad Sci U S A.* 1997. 94(17), 8994–9. <https://doi.org/10.1073/pnas.94.17.8994> PMID: 9256423
74. Schafer B, Wilde B, Massardo DR, Manna F, Giudice LD, Wolf K. A mitochondrial group I intron in fission yeast encodes a maturase and is mobile in crosses. *Curr Genet.* 1994. 25, 33–341. <https://doi.org/10.1007/BF00351487> PMID: 8082176
75. Monteilhet C, Dziadkowiec D, Szczepanek T, Lazowska J. Purification and characterization of the DNA cleavage and recognition site of I-Scal mitochondrial group I intron encoded endonuclease produced in *Escherichia coli*. *Nucleic Acids Res.* 2000. 28(5), 1245–1251. <https://doi.org/10.1093/nar/28.5.1245> PMID: 10666469
76. Van Ommen GJB, Boer PH, Groot GSP, de Haan M, Roosendaal E, Grivell LA, et al. Mutations affecting RNA splicing and the interaction of gene expression of the yeast mitochondrial loci *cob* and *oxi-3*. *Cell.* 1980. 20(1), 173–183. [https://doi.org/10.1016/0092-8674\(80\)90245-7](https://doi.org/10.1016/0092-8674(80)90245-7) PMID: 6993008
77. Chevalier BS, Stoddard BL. Homing endonucleases: structural and functional insight into the catalysts of intron/intein mobility. *Nucleic Acids Res.* 2001. 29(18): 3757–3774. <https://doi.org/10.1093/nar/29.18.3757> PMID: 11557808
78. Zubaer A, Wai A, Hausner G. The fungal mitochondrial Nad5 pan-genic intron landscape, *Mitochondrial DNA Part A.* 2019. 30(8), 835–842. <https://doi.org/10.1080/24701394.2019.1687691> PMID: 31698975
79. Al-Reedy RM, Malireddy R, Dillman CB, Kennell JC. Comparative analysis of *Fusarium* mitochondrial genomes reveals a highly variable region that encodes an exceptionally large open reading frame. *Fungal Genet. Biol.* 2012; 49(1), 2–14. <https://doi.org/10.1016/j.fgb.2011.11.008> PMID: 22178648
80. Torriani SFF, Goodwin SB, Kema GHJ, Pangilinan JL, McDonald BA. Intraspecific comparison and annotation of two complete mitochondrial genome sequences from the plant pathogenic fungus *Mycosphaerella graminicola*. *Fungal Genetics and Biology.* 2008; 45(5)628–637. <https://doi.org/10.1016/j.fgb.2007.12.005> PMID: 18226935

81. Ambrosio AB, Nascimento LC, Oliveira BV, Teixeira PJPL, Tiburcio RA, Thomazella DPT et al. Global analyses of *Ceratocystis cacaofunesya* mitochondria: from genome to proteome. *BMC Genomics* 2013; 14(91). <https://doi.org/10.1186/1471-2164-14-91> PMID: 23394930
82. Zhang Y, Zhang S, Zhang G, Liu X, Wang C, Xu J. Comparison of mitochondrial genomes provides insights into intron dynamics and evolution in the caterpillar fungus *Cordyceps militaris*. *Fungal Genet. Biol.* 2015; 77, 95–107. <https://doi.org/10.1016/j.fgb.2015.04.009> PMID: 25896956
83. Aguilera G, De Vienne DM, Ross ON, Hood ME, Giraud T, Petit E, et al. High variability of mitochondrial gene order among fungi. *Genome Biol. Evol.* 2014; 6(2), 451–465. <https://doi.org/10.1093/gbe/evu028> PMID: 24504088
84. Robicbeau BM, Young AP, Labutti K, Grigoriev IV, Walker AK. The complete mitochondrial genome of the conifer needle endophyte, *Phialocephala scopiformis* DAOMC 229536 confirms evolutionary division within the fungal *Phialocephala fortinii* s.l.—*Acephala appalanata* species complex. *Fungal Biol.* 2017; 121(3), 212–221. <https://doi.org/10.1016/j.funbio.2016.11.007> PMID: 28215349
85. Shen XY, Li T, Chen S, Fan L, Gao J, Hou CL. Characterization and phylogenetic analysis of the mitochondrial genome of *Shiraia bambusicola* reveals special features in the order of Pleosporales. *PLoS One.* 2015; 10(3):e0116466. <https://doi.org/10.1371/journal.pone.0116466> PMID: 25790308
86. Wang P, Sha T, Zhang Y, Cao Y, Mi F, Liu C et al. Frequent heteroplasmy and recombination in the mitochondrial genomes of the basidiomycete mushroom *Thelephora ganbajun*. *Sci. Rep.* 2017;9; 7(1), 1626. <https://doi.org/10.1038/s41598-017-01823-z> PMID: 28487526
87. Li Q, Chen C, Xiong C, Jin X, Chen Z, Huang W. Comparative mitogenomics reveals large-scale gene rearrangements in the mitochondrial genome of two *Pleurotus* species. *Appl. Microbiol. Biotechnol.* 2018; 102(14), 6143–6153. <https://doi.org/10.1007/s00253-018-9082-6> PMID: 29799088
88. Tang G, Zhang C, Ju Z, Zheng S, Wen Z, Xu S, et al. The mitochondrial membrane protein FgLetm1 regulates mitochondrial integrity, production of endogenous reactive oxygen species and mycotoxin biosynthesis in *Fusarium graminearum*. *Mol. Plant Pathol.* 2018, 19(7), 1595–1611. <https://doi.org/10.1111/mpp.12633> PMID: 29077257
89. Zoschke R, Nakamura M, Liere K, Sugiura M, Börner T, Schmitz-Linneweber C. An organellar maturase associates with multiple group II introns. *Natl Acad Sci U S A.* 2010; 107:3245–3250. <https://doi.org/10.1073/pnas.0909400107> PMID: 20133623
90. Keren I, Bezawork-Geleta A, Kolton M, Maayan I, Belausov E, Levy M, et al. AtnMat2, a nuclear-encoded maturase required for splicing of group-II introns in *Arabidopsis* mitochondria. *RNA.* 2009; 15:2299–2311. <https://doi.org/10.1261/rna.1776409> PMID: 19946041
91. Jia W, Higgs PG. Codon usage in mitochondrial genomes: distinguishing context-dependent mutation from translational selection. *Mol. Biol. Evol.* 2008. 25(2). 339–351, <https://doi.org/10.1093/molbev/msm259> PMID: 18048402